Mechanism of oxidative conversion of Amplex® Red to resorufin: pulse radiolysis and enzymatic studies.

[1]Dawid Dębski, [1]Renata Smulik, [2]Jacek Zielonka*, [1]Bartosz Michałowski, [1]Małgorzata Jakubowska, [1]Karolina Dębowska, [1]Jan Adamus, [1]Andrzej Marcinek, [2]Balaraman Kalyanaraman, [1]Adam Sikora*

[1]Institute of Applied Radiation Chemistry, Lodz University of Technology, Lodz, Poland

[2]Department of Biophysics and Free Radical Research Center, Medical College of Wisconsin, Milwaukee, Wisconsin, United States

SUPPLEMENTAL DATA

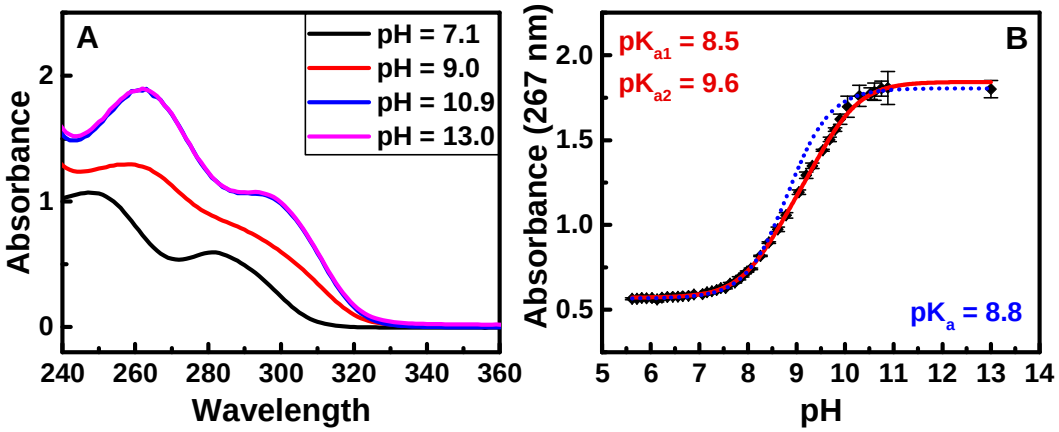

Supplemental Figure S1 A: UV-vis absorption spectra of 100 µM Amplex® Red dissolved in a solution containing 10% CH_3CN and 200 mM aqueous phosphate buffer in the indicated pH range. **B:** Determination of pK_a values of Amplex® Red in aqueous solution. Absorbance was measured at 267 nm. Non-linear fitting considered one (blue) or two (red) pK_as.

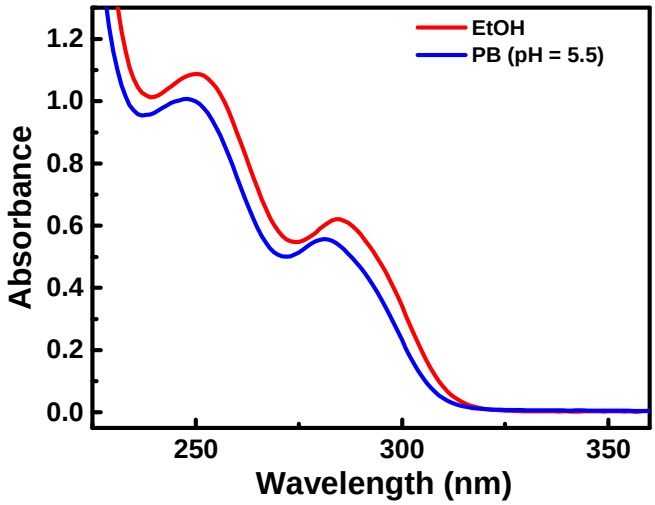

Supplemental Figure S2 UV-vis absorption spectra of 100 µM of Amplex® Red in ethanol (EtOH) and aqueous phosphate buffer (PB) at pH 5.5.

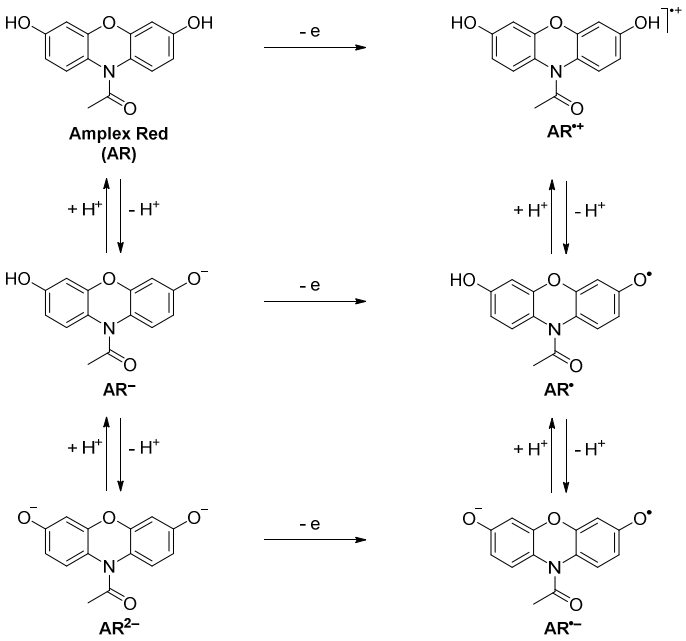

Supplemental Figure S3 The chemical structures of possible acid-base forms of Amplex® Red and its one-electron oxidation products.

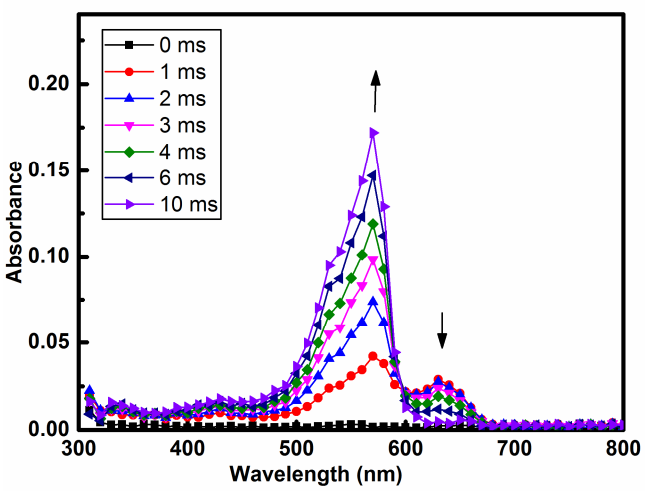

Supplemental Figure S4. Transient absorption spectra obtained by pulse radiolysis of Amplex® Red (200 µM) in a N_2O-saturated aqueous solution containing 50 mM $NaNO_3$, 10 mM $NaNO_2$, 50 mM phosphate buffer (pH = 7.4) and 5% CH_3CN. Arrows indicate the direction of spectral evolution over time. Administered radiation dose per pulse was approx. 50 Gy.

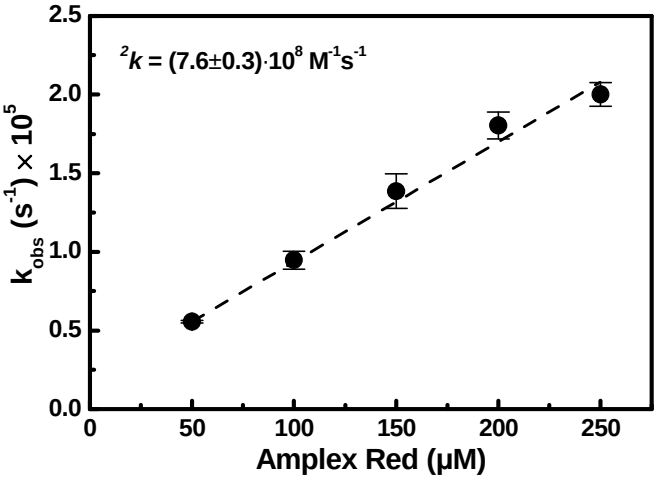

Supplemental Figure S5 The dependence of the pseudo-first order rate constant of the reaction of Amplex® Red with carbonate radical anion on the initial concentration of Amplex® Red. Incubation mixtures contained 0.25 M Na_2CO_3, 0.25 M $NaHCO_3$ (pH 10.3), 10% CH_3CN, 50-250 μM Amplex® Red and were saturated with N_2O prior to irradiation with 7 ns electron pulse (15 Gy dose). The reaction kinetics was monitored at 370 nm.

Cyclic Voltammetry. The determination of redox properties of Amplex® Red was performed with the use of Autolab PGSTAT 30 (Eco Chemie BV, Netherlands) potentiostat/galvanostat equipped with working platinum electrode (0.28 cm^2), auxiliary platinum electrode (0.56 cm^2) and Ag/Ag^+ reference electrode. Electrolyte consisted of 0.01 M $AgNO_3$, 0.1 M tetrabutylammonium perchlorate/CH_3CN, Amplex® Red concentration was 500 µM. Scans were performed at 100 mV/s scan rate in the range between -0.5 to 1.25 V.

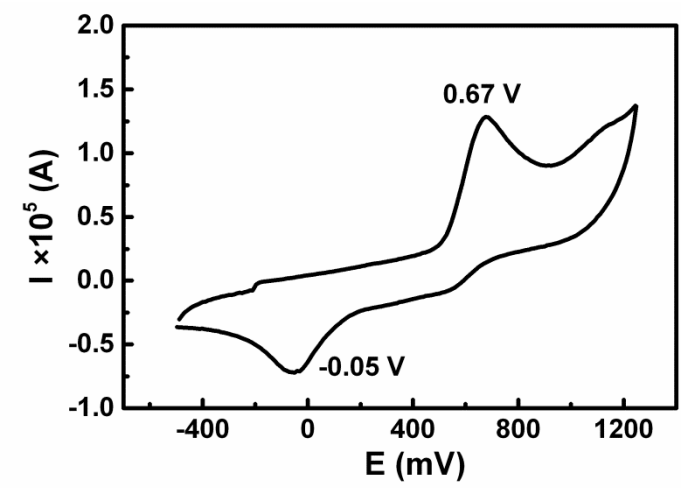

Supplemental Figure S6. Cyclic voltammogram of the solution of 500 µM Amplex® Red containing 0.01 M $AgNO_3$ and 0.1 M tetrabutylammonium perchlorate in CH_3CN. Scan rate was equal to 100 mV/s in the range between -0.5 to 1.25 V.

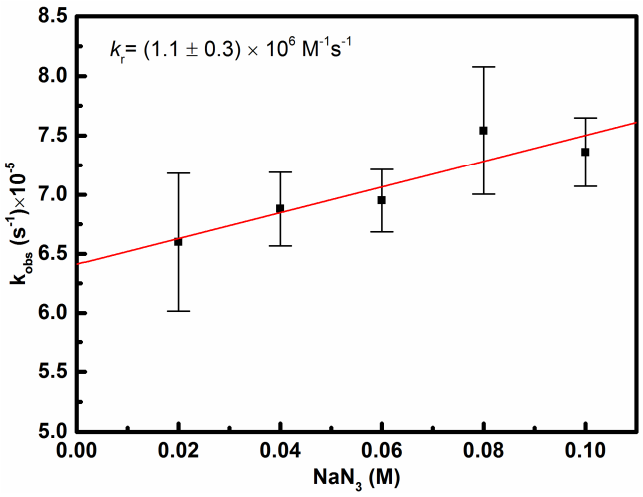

Supplemental Figure S7. The dependence of the pseudo-first order rate constant of the buildup of Amplex® Red radical, formed in the reaction with azidyl radical, on the concentration of NaN_3. Incubation mixtures contained 0.02-0.1 M NaN_3, 50 mM phosphate buffer (pH = 7.5), 5% CH_3CN, 250 µM Amplex® Red and were saturated with N_2O prior to irradiation with 7 ns electron pulse (15 Gy dose). The reaction kinetics was monitored at 370 nm.

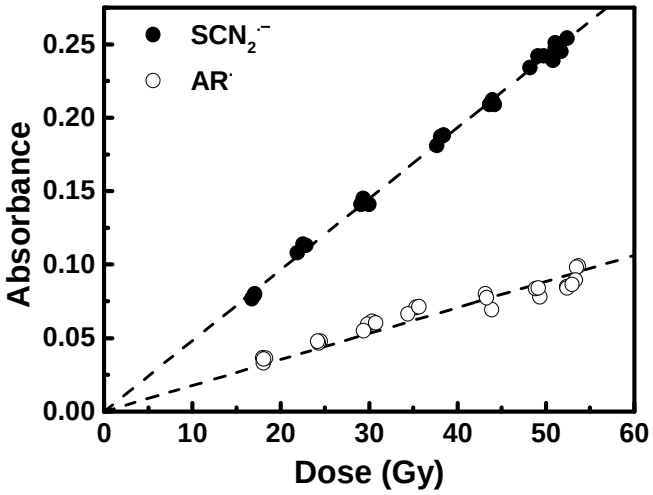

Supplemental Figure S8. The dependence of the measured absorbance at 475 nm ($SCN_2^{\cdot-}$, filled circles) and at 820 nm ($AR^{\bullet}$, empty circles) on the radiation dose upon radiolysis of the N_2O saturated solutions containing 0.01 M KSCN, 10% CH_3CN or 50 µM Amplex® Red, 0.01 M NaN_3, 10% respectively. Absorbance was measured at 500 ns for KSCN solution and 8 µs for Amplex® Red solution after the electron pulse.

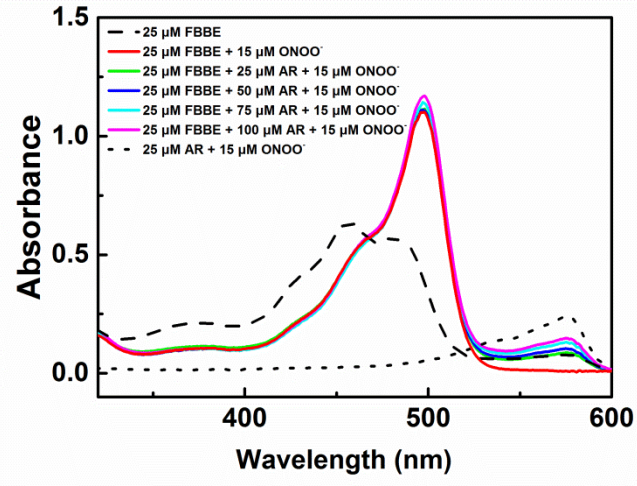

Supplemental Figure S9 UV-vis absorption spectra of the solutions containing 25 μM FBBE probe, 0-100 μM Amplex® Red, 50 mM phosphate buffer (pH 7.4), 100 μM dtpa, 20% CH_3CN, after the addition of 15 μM $ONOO^-$ (solid lines, different colors). The spectra were recorded at 10 minutes after the addition of peroxynitrite.

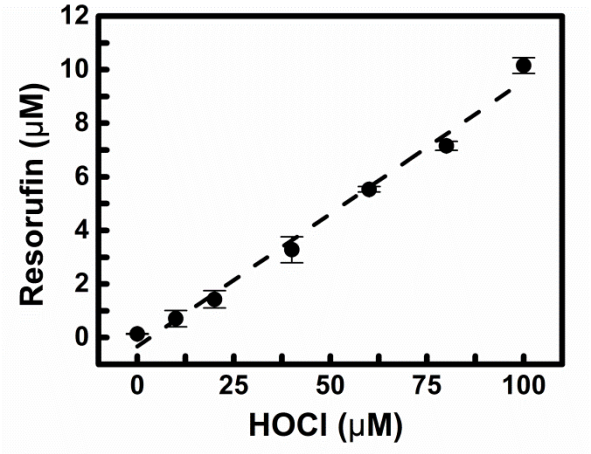

Supplemental Figure S10. The amount of resorufin formed after addition of 0-100 μM of HOCl to the solution containing 50 μM Amplex® Red, 50 mM PB (pH 7.4), 10% CH_3CN. Resorufin concentration was calculated from the absorbance measured at 573 nm assuming ε_{573nm}= 6.3×10^4 $M^{-1}cm^{-1}$.

Quantum Chemical Calculations

Geometric structures of all species were optimized according to UB3LYP density functional method [1] with the 6-31++g(d,p) basis set implemented into the Gaussian 09 program [2]. The angle between planes calculated for two aromatic rings was determined with the use of CCDC Mercury program.

Results

By performing the quantum chemical calculations an interesting aspect of mechanistic scheme of one-electron oxidation of Amplex® Red was delivered (Fig. S11). The initial angle between two aromatic rings of Amplex® Red structure (1) was calculated to be approximately 143.8°. In the optimized structure of Amplex® Red neutral radical (2) the planar angle is wider (149.3°) and the acetyl group is slightly rotated. The two-electron oxidation intermediate formed after disproportionation the radicals (3) shows a flat structure (178.2°) nearly identical to the final product, resorufin, with both aromatic rings lying in one plane and with the acetyl group positioned perpendicularly to the plane. The length of the bond between the nitrogen atom and the carbon atom from the acetyl group has also changed from the initial value of 1.390 Å to 1.547 Å in the course of reaction, lowering the energy necessary for acetyl group dissociation.

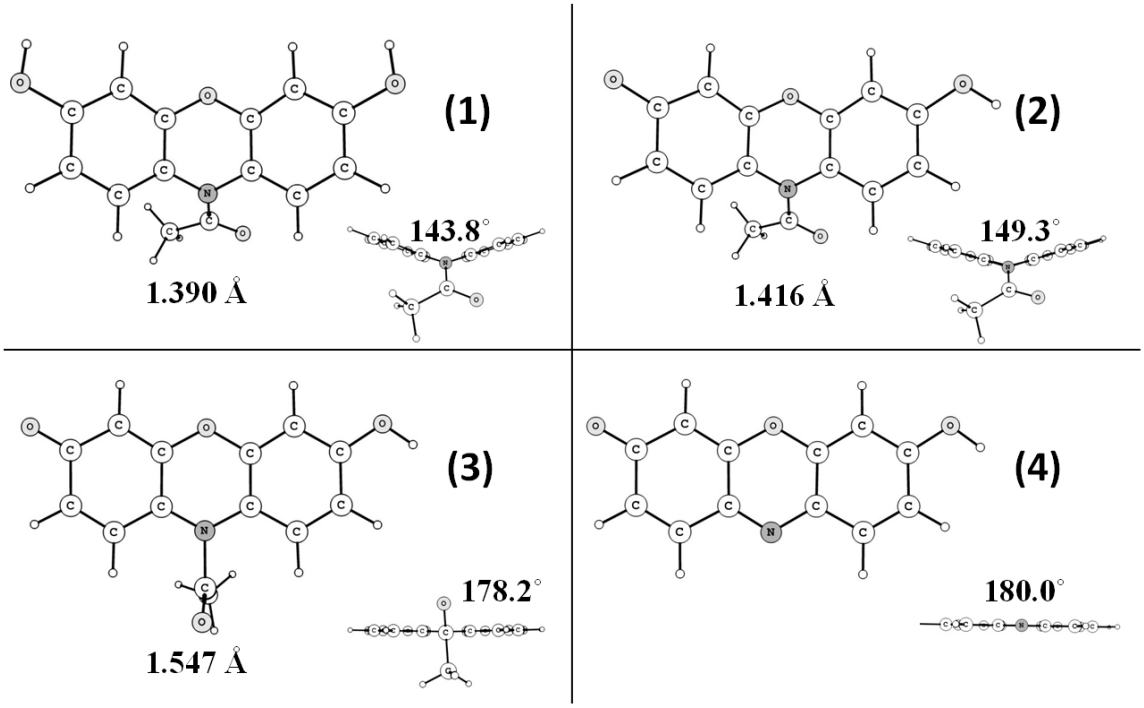

Supplemental Figure S11. Optimized geometric structures of Amplex Red, resorufin and the proposed intermediates, optimized according to UB3LYP density functional method with the 6-31++g(d,p) basis set. Numbers in parentheses correspond to the structures shown in Figure 11.

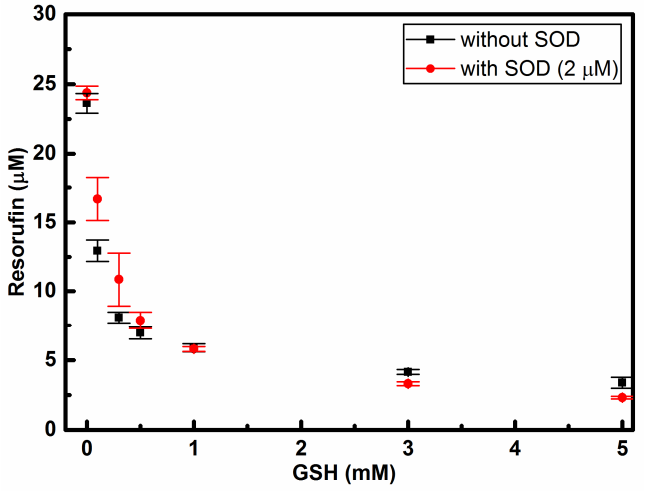

Supplemental Figure S12. The effect of glutathione and SOD on the yield of resorufin formed from Amplex® Red in the aqueous solutions containing 100 μM AR, 25 μM H_2O_2, 50 mM phosphate buffer (pH = 7.4), 5% CH_3CN, 0-5 mM GSH and 2 μM SOD (if indicated).

Reference List

[1] Becke A.D. Density-functional thermochemistry. III. The role of exact exchange. *J Chem Phys* ;**98**:5648-52;1993

[2] Gaussian 09, Revision A.02, Frisch, M. J.; Trucks, G. W.; Schlegel, H. B.; Scuseria, G. E.; Robb, M. A.; Cheeseman, J. R.; Scalmani, G.; Barone, V.; Mennucci, B.; Petersson, G. A.; Nakatsuji, H.; Caricato, M.; Li, X.; Hratchian, H. P.; Izmaylov, A. F.; Bloino, J.; Zheng, G.; Sonnenberg, J. L.; Hada, M.; Ehara, M.; Toyota, K.; Fukuda, R.; Hasegawa, J.; Ishida, M.; Nakajima, T.; Honda, Y.; Kitao, O.; Nakai, H.; Vreven, T.; Montgomery, J. A., Jr.; Peralta, J. E.; Ogliaro, F.; Bearpark, M.; Heyd, J. J.; Brothers, E.; Kudin, K. N.; Staroverov, V. N.; Kobayashi, R.; Normand, J.; Raghavachari, K.; Rendell, A.; Burant, J. C.; Iyengar, S. S.; Tomasi, J.; Cossi, M.; Rega, N.; Millam, J. M.; Klene, M.; Knox, J. E.; Cross, J. B.; Bakken, V.; Adamo, C.; Jaramillo, J.; Gomperts, R.; Stratmann, R. E.; Yazyev, O.; Austin, A. J.; Cammi, R.; Pomelli, C.; Ochterski, J. W.; Martin, R. L.; Morokuma, K.; Zakrzewski, V. G.; Voth, G. A.; Salvador, P.; Dannenberg, J. J.; Dapprich, S.; Daniels, A. D.; Farkas, Ö.; Foresman, J. B.; Ortiz, J. V.; Cioslowski, J.; Fox, D. J. Gaussian, Inc., Wallingford CT, 2009.